

Learning incomplete factorization preconditioners for GMRES

Paul Häusner^{*1}, Aleix Nieto Juscafresa^{*1}, and Jens Sjölund¹

¹Department of Information Technology, Uppsala University, Sweden
{paul.hausner, aleix.nieto-juscafresa, jens.sjolund}@it.uu.se

Abstract

In this paper, we develop a data-driven approach to generate incomplete LU factorizations of large-scale sparse matrices. The learned approximate factorization is utilized as a preconditioner for the corresponding linear equation system in the GMRES method. Incomplete factorization methods are one of the most commonly applied algebraic preconditioners for sparse linear equation systems and are able to speed up the convergence of Krylov subspace methods. However, they are sensitive to hyper-parameters and might suffer from numerical breakdown or lead to slow convergence when not properly applied. We replace the typically hand-engineered algorithms with a graph neural network-based approach that is trained against data to predict an approximate factorization. This allows us to learn preconditioners tailored for a specific problem distribution. We analyze and empirically evaluate different loss functions to train the learned preconditioners and show their effectiveness to decrease the number of GMRES iterations and improve the spectral properties on our synthetic dataset. The code is available at <https://github.com/paulhausner/neural-incomplete-factorization>.

1 Introduction

The GMRES algorithm is one of the most popular iterative methods to solve large-scale and sparse linear equation systems of the form $\mathbf{Ax} = \mathbf{b}$. Throughout the paper, we assume the system matrix \mathbf{A} to be real-valued and full rank. Therefore, the unique solution $\mathbf{A}^{-1}\mathbf{b}$ exists. However, inverting the matrix directly, or equivalently computing a full matrix factorization, scales computationally poorly and suffers from numerical instabilities. Instead, iterative Krylov subspace methods (such as GMRES) which refine an approximation of the solution in each step are the most common approach to solving problems of this form. The convergence of these methods highly depends on the conditioning and singular value distribution of the system matrix. Therefore, the choice of appropriate preconditioner – designed to improve the system properties – is critical to obtain a fast and accurate solution for the equation system [1].

One of the most common choices of preconditioners is the incomplete LU factorization (ILU). As the name suggests, the matrix \mathbf{A} is factorized but not all elements of the factorization are computed to decrease the storage and computational time [2, 3]. In this work, we replace the classical computation of the LU factors with a graph neural network (GNN). We train the GNN to predict the corresponding incomplete factors of the matrix directly by training against data. The main contributions of our paper are the following:

- We design a GNN model and train it to output a non-singular incomplete LU factorization.
- We theoretically analyze existing loss functions from the literature and showcase their connection to large and small singular values.
- Based on these insights, we derive a novel loss function to train learned preconditioners that combines the benefits of previous approaches.

In numerical experiments, we showcase the effectiveness of our model to reduce GMRES iterations in combination with the different loss functions and validate the theoretical results on a synthetic dataset.

Related work Most similar to our work, Häusner et al. [4] and Li et al. [5] both learn an incomplete factorization for the conjugate gradient method. Trifonov et al. [6] extend this to combine data-driven and classical algorithms by correcting the output of the incomplete Cholesky factorization with a learned component. However, all of these methods assume the matrix to be symmetric and positive definite and utilize the incomplete Cholesky factorization as the underlying preconditioning technique. In contrast, rather focus on the more general incomplete LU factorization, which does not require positive definiteness or symmetry, within the GMRES algorithm.

In previous work, Chen [7] instead proposes directly estimating the inverse of the matrix using a non-linear neural network as a preconditioner, requiring the use of the flexible GMRES method, which has a more complex convergence behavior. However, the proposed method requires retraining for each new problem. In contrast, we propose leveraging the similarity within a class of linear equation systems to first train the model offline and then generate preconditioners for new problems with a negligible computational overhead during inference time.

^{*}Joint first author.

For the class of sparse approximate inverse preconditioner, Bánkestad et al. [8] learn the sparsity pattern of the approximate inverse matrix. Li et al. [9] instead propose to learn auto-encoder-based generative models to generate preconditioners. In contrast, this paper only focuses on learning factorized preconditioners that allow easy inversion.

2 Background

We first briefly introduce the GMRES algorithm and focus in particular on the design choice of preconditioners. Then, we describe graph neural networks which we use to parameterize the mapping to learn data-driven preconditioners.

2.1 GMRES algorithm

We focus on the GMRES algorithm [10], a popular and widely adopted iterative Krylov subspace method to solve general linear equation systems of the form $\mathbf{Ax} = \mathbf{b}$ where \mathbf{A} is a $n \times n$ non-singular matrix denoted by the set $\text{GL}(n, \mathbb{R})$. The core idea of Krylov subspace methods is to iteratively refine the solution to the problem starting from an initial guess \mathbf{x}_0 . At each iteration, the approximate solution is updated by minimizing the Euclidean norm of the residual within the corresponding Krylov subspace:

$$\mathbf{x}_k = \arg \min_{\mathbf{x} \in \mathbf{x}_0 + \mathcal{K}_k(\mathbf{A}, \mathbf{r}_0)} \|\mathbf{b} - \mathbf{Ax}\|_2, \quad (1)$$

where the k -th Krylov subspace $\mathcal{K}_k(\mathbf{A}, \mathbf{r}_0) = \text{span}\{\mathbf{r}_0, \mathbf{Ar}_0, \mathbf{A}^2\mathbf{r}_0, \dots, \mathbf{A}^{k-1}\mathbf{r}_0\}$ of \mathbf{A} is generated by the initial residual $\mathbf{r}_0 = \mathbf{b} - \mathbf{Ax}_0$ [1]. The new approximation \mathbf{x}_k builds on the previous solution \mathbf{x}_{k-1} by efficiently computing it within a progressively larger Krylov subspace by constructing the solution in a progressively larger subspace that captures more of the action of the matrix \mathbf{A} on the residual. This expanding subspace offers more directions to approximate the solution, improving the conditioning and accuracy of the minimization problem over iterations. The efficiency arises because \mathbf{x}_k is found by solving a smaller, reduced system in the subspace rather than the original larger system. The GMRES algorithm is guaranteed to find the exact solution to the linear equation system in at most n steps.

Each iteration consists of two main steps. In the first step of the algorithm, an orthonormal basis for the subspace \mathcal{K}_k is computed. This can be achieved, for example, using Arnoldi’s algorithm which is based on the Gram-Schmidt procedure. In the second step, an unconstrained least squares problem is solved via the QR factorization of the subspace basis obtained in the first step. Based on this, the solution of Equation (1) can be constructed efficiently. The detailed algorithm is shown in Appendix A.

Preconditioning Arguably, the most important design choice for any Krylov subspace method is the choice of preconditioner. The goal of preconditioning is to replace the original linear equation system with a new preconditioned system that exhibits a better clustering of singular values, which in turn leads to faster convergence of the iterative scheme [11]. For a non-singular and easy-to-invert matrix \mathbf{P} , the linear equation system $\mathbf{AP}^{-1}\mathbf{y} = \mathbf{b}$ is solved instead of the original problem. The solution to the original problem is then given by $\mathbf{x} = \mathbf{P}^{-1}\mathbf{y}$.¹ Constructing a preconditioner involves trading off the time required to compute the preconditioner itself and the resulting speed up in the iterative scheme [2]. Since the original system \mathbf{A} is typically sparse, we restrict the preconditioning matrix \mathbf{P} to be subject to sparsity constraints as well.

Algebraic preconditioners do not assume any additional problem information and compute the preconditioning matrix solely based on the structure and values of the matrix \mathbf{A} in contrast to methods taking into account the underlying problem domain.

In the simplest case, the Jacobi preconditioner approximates \mathbf{P} using a diagonal matrix. More advanced methods such as incomplete factorizations or the Gauss-Seidel method compute approximate factorizations of the original system \mathbf{A} which implicitly give rise to preconditioners as they allow efficient inversions [2, 12]. Most commonly, the approximation utilizes triangular factorizations since efficient inversion in at most $\mathcal{O}(n^2)$ operations can be achieved and sparsity can be exploited [13]. However, It is also possible to approximate the matrix \mathbf{P}^{-1} directly [14].

2.2 Graph neural networks

Graph neural networks (GNNs) are a recently popularized family of neural network architectures designed to process data represented on unstructured grids or graphs [15]. A graph is a tuple $\mathcal{G} = (\mathcal{V}, \mathcal{E})$ consisting of vertices (or nodes) \mathcal{V} and a bivariate relation of edges $\mathcal{E} \subseteq \mathcal{V} \times \mathcal{V}$. With slight abuse of notation, we refer to the edge features of the edge $e = (i, j) \in \mathcal{E}$ as $\mathbf{e}_{ij} \in \mathbb{R}^m$ and node features of node $i \in \mathcal{V}$ as $\mathbf{n}_i \in \mathbb{R}^k$. The message-passing framework updates the initial edge and node features – representing the input data – in each layer l as follows:

$$\mathbf{e}_{ij}^{l+1} = \psi_{\theta}(\mathbf{e}_{ij}^l, \mathbf{n}_i^l, \mathbf{n}_j^l) \quad (2a)$$

$$\mathbf{m}_i^{l+1} = \bigoplus_{j \in \mathcal{N}(i)} \mathbf{e}_{ji}^{l+1} \quad (2b)$$

$$\mathbf{n}_i^{l+1} = \phi_{\theta}(\mathbf{n}_i^l, \mathbf{m}_i^{l+1}). \quad (2c)$$

Here, the functions ψ and ϕ , which update the node and edge features respectively, are parameterized by

¹Here, right preconditioning is used, but other formulations use left- or split-preconditioning instead often leading to similar but not equivalent results.

neural networks, and their respective parameters θ are learned during the model training. Note that all feature vectors within a single layer must be of the same size, although the embedding size can vary between different layers. Equation (2b) shows the aggregation of the adjacent edges features for each vertex $i \in \mathcal{V}$ called the neighborhood $\mathcal{N}(i)$. Any permutation invariant function \oplus , such as sum and mean, can be utilized for this aggregation step [16].

3 Method

Throughout this paper, we are interested in solving many linear equation systems that share an underlying structure. Instead of having direct access to a probability distribution over problems, we obtain a dataset D with a finite number of samples $\mathbf{A}_1, \mathbf{A}_2, \dots, \mathbf{A}_{|D|}$. As previously stated, we assume each \mathbf{A}_i to be square, non-singular and sparse.

3.1 Network architecture

The goal of this paper is to learn a mapping f_θ , parameterized by a graph neural network, that takes a non-singular matrix $\mathbf{A} \in \text{GL}(n, \mathbb{R})$ as input and outputs the corresponding preconditioner \mathbf{P} for the equation system. In order to ensure that the preconditioning system is easily invertible – such that we can apply it within the GMRES algorithm – we learn the LU factorization of the preconditioner \mathbf{P} instead, by mapping \mathbf{A} to two real matrices \mathbf{L} and \mathbf{U} . The output matrices are lower and upper triangular, respectively, with non-zero diagonal entries to ensure their invertibility as discussed later. For notational simplicity, we do not explicitly mention the dependence of the factors on the original matrix \mathbf{A} and the neural network parameters θ when the relationship is clear from the context.

Sparsity Further, the two output factors, \mathbf{L} and \mathbf{U} , are subject to sparsity constraints. Similar to incomplete LU factorization methods without fill-ins ILU(0), we enforce the same sparsity patterns to the elements of \mathbf{L} and \mathbf{U} as the original matrix \mathbf{A} . This constraint is directly encoded in the network architecture as we discuss next.

Network parameterization To parameterize the function f_θ that outputs the preconditioner, we exploit the strong connection of matrices and linear algebra with graph neural networks [17, 18].

We treat the system \mathbf{A} as the adjacency matrix of a corresponding graph that we use directly within the message-passing framework. This transformation is known in the literature as Coates graph representation is depicted in Figure 1 [19]. Similar to Häusner et al. [4] and Tang et al. [20], we use node features describing the structural properties of the corresponding rows and columns of the matrix. We

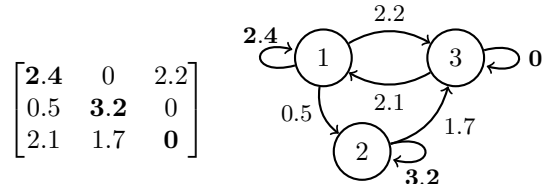


Figure 1. Non-symmetric matrix \mathbf{A} (left) and the corresponding sparse Coates graph representation (right). Additionally to the non-zero elements in the matrix, the graph has been modified by adding edges for all missing diagonal elements, corresponding to self-loops.

use the non-zero elements of \mathbf{A} as the corresponding edge features of the graph.

Compared to previous approaches which only output a single lower triangular factor, our model outputs two separate matrices \mathbf{L} and \mathbf{U} . Häusner et al. [4] add positional encodings about the output matrix by explicitly changing the Coates graph representation. This allows them to output the lower triangular factor as the message passing is only executed over this set of edges. In contrast, we add positional encodings to the input data by adding an additional edge feature to each directed edge in the graph. This indicates whether the final output embedding of the corresponding edge belongs to the upper- or lower-triangular part (± 1 respectively) but does not change the underlying graph structure used for message passing.

Invertibility We require the predicted factors \mathbf{L} and \mathbf{U} of the preconditioner obtained from the forward pass through the model to be invertible in order to obtain a valid preconditioner for the GMRES method during inference. Therefore, we need to enforce non-zero elements on each diagonal.

Since the input matrix \mathbf{A} is not guaranteed to have non-zero diagonal elements, we add the corresponding edges to the graph if necessary before the message passing. This is visualized for the matrix element A_{33} in Figure 1.

However, it is still possible that the output of the GNN results in a singular matrix as the final edge representations, obtained from message passing, can result in zero diagonal elements. Through additional measures, we avoid this in both factors and enforce non-singularity. Inspired by the classical LU factorization, we enforce unit diagonal elements for the \mathbf{U} factor. For the diagonal elements in the lower triangular factor \mathbf{L} we are using the activation function

$$\zeta(x) = \begin{cases} x, & \text{if } |x| > \epsilon, \\ \epsilon, & \text{if } 0 \leq x \leq \epsilon, \\ -\epsilon, & \text{if } -\epsilon \leq x < 0, \end{cases} \quad (3)$$

for a chosen small value $\epsilon = 10^{-4}$. This guarantees

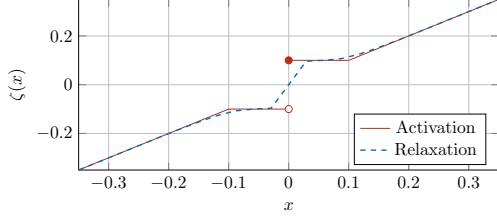


Figure 2. Plot of the activation function (3) for $\epsilon = 0.1$ and the corresponding relaxation (4).

that the output matrix \mathbf{L} is invertible as diagonal elements with a small magnitude are shifted away from zero. However, this function is discontinuous at $x = 0$ making it difficult to optimize using gradient-based methods. Therefore, we use the following continuous approximation of the activation function

$$\hat{\zeta}(x) = x \cdot \left(1 + \exp \left(- \left| \frac{4x}{\epsilon} \right| + 2 \right) \right) \quad (4)$$

during training. The plots for the activation function and the proposed relaxation are shown in Figure 2.

3.2 Model training

The goal of the learned preconditioner $\mathbf{P} = \mathbf{L}\mathbf{U}$ is to improve the spectral properties of the preconditioned linear equation system $\mathbf{A}\mathbf{P}^{-1}$. However, directly optimizing the condition number κ of the system as suggested by Sappl et al. [21] is computationally infeasible for large-scale problems. For computational tractability, we are also not taking the whole spectrum of the equation system into account but concentrate on the edges of the spectrum. In other words, we consider only the largest and smallest singular values of the preconditioned equation system.

Lemma 1 *The largest singular value of the matrix $\mathbf{P}^{-1}\mathbf{A}$ is upper bounded by the Frobenius norm: $\sigma_{\max}(\mathbf{A}\mathbf{P}^{-1}) \leq \epsilon^{-1} \|\mathbf{A} - \mathbf{P}\|_F + 1$.*

Here, ϵ is the hyper-parameter of the preconditioner chosen in Equation (3). Further, we can estimate the Frobenius norm using Hutchinson’s trace estimator [22] which allows us to express the loss to minimize the upper bound on the largest singular value of the system in the following form:

$$\mathcal{L}_{\max}(\mathbf{P}; \mathbf{A}) = \|\mathbf{A}\mathbf{w} - \mathbf{P}\mathbf{w}\|_2^2, \quad (5)$$

where \mathbf{w} is a standard normal distributed vector. This loss function was first suggested by Häusser et al. [4] as an approximation of the Froebnius norm.

Lemma 2 *The smallest singular value of $\mathbf{A}\mathbf{P}^{-1}$ is lower bounded by the following inequalities: $\sigma_{\min}(\mathbf{A}\mathbf{P}^{-1}) \geq \|\mathbf{P}\mathbf{A}^{-1}\|_F^{-1} \geq (\|\mathbf{P}\mathbf{A}^{-1} - \mathbf{I}\|_F + 1)^{-1}$*

Based on this lemma, we obtain the following loss function² by using a similar approximation as in the previous step and optimizing over the inverse:

$$\mathcal{L}_{\min}(\mathbf{P}; \mathbf{A}) = \|\mathbf{P}\mathbf{A}^{-1}\mathbf{w} - \mathbf{w}\|_2^2. \quad (6)$$

The drawback of this loss is that it requires computing $\mathbf{A}^{-1}\mathbf{w}$ during training. In other words, we need to solve many potentially ill-conditioned linear systems in order to train the learned preconditioner. Chen [7] proposes a similar loss function and approximates the solutions to the linear equation system instead using Arnoldi’s method.

To maintain computational efficiency we can make use of a supervised dataset instead, consisting of tuples $(\mathbf{A}_i, \mathbf{x}_i, \mathbf{b}_i)$ such that $\mathbf{A}_i\mathbf{x}_i = \mathbf{b}_i$. This requires us to solve each training problem only once which can be computed beforehand in an offline fashion. We replace the standard distributed samples \mathbf{w} in Equation (6) with the available training samples. This avoids solving problem instances during training but leads to a biased approximation of the previous loss function:

$$\hat{\mathcal{L}}_{\min}(\mathbf{P}; \mathbf{A}) = \|\mathbf{P}\mathbf{A}^{-1}\mathbf{b} - \mathbf{b}\|_2^2 = \|\mathbf{P}\mathbf{x} - \mathbf{b}\|_2^2. \quad (7)$$

Li et al. [5] originally suggested this loss function as an approximation of the Frobenius norm loss and motivate it by including inductive bias from the training data. Later, Trifonov et al. [6] obtain the same approximation by reweighting of Equation (5) with the inverse matrix. They conjecture the connection of the loss function with small singular values and, further, empirically show that minimizing this loss increases the smallest singular value of the preconditioned system.

By combining the two previous loss functions from Equation (6) and the unregularized version of Equation (5), we introduce a novel combined loss with the goal to further improve the conditioning by taking into account both ends of the spectrum. The combined loss function and the approximation using a supervised dataset similar to Equation (7) are

$$\begin{aligned} \mathcal{L}_{\text{com}}(\mathbf{P}; \mathbf{A}) &= \|\mathbf{A}\mathbf{w} - \mathbf{P}\mathbf{w}\|_2^2 + \alpha \|\mathbf{P}\mathbf{A}^{-1}\mathbf{w}\|_2^2 \\ &\approx \|\mathbf{A}\mathbf{w} - \mathbf{P}\mathbf{w}\|_2^2 + \alpha \|\mathbf{P}\mathbf{x}\|_2^2, \end{aligned} \quad (8)$$

where α is a hyper-parameter chosen to balance the two individual loss terms. During the training, we are minimizing the empirical risk over the corresponding unsupervised or supervised dataset to learn the parameters:

$$\hat{\theta} \in \arg \min_{\theta} \sum_{i=1}^{|D|} \mathcal{L}(\mathbf{P}_{\theta}; \mathbf{A}_i, \mathbf{x}_i, \mathbf{b}_i). \quad (9)$$

The proofs for the lemmas and the connection of the loss functions to previous methods from the literature can be found in Appendix C.

²By convention, we always minimize the loss function.

Table 1. Average performance of classical and data-driven preconditioners with different loss functions evaluated on 10 test samples. We show the conditioning of the right-preconditioned system $\mathbf{A}\mathbf{P}^{-1}$ as well as the convergence of the GMRES algorithm in terms of the total time required to compute the preconditioner and solve the systems and the number of iterations. For the unpreconditioned method, we compute the loss for $\mathbf{P} = \mathbf{I}$. Arrows indicate if higher or lower is better. The best performance is marked in bold.

	Method	$\sigma_{\min} \uparrow$	$\sigma_{\max} \downarrow$	$\kappa \downarrow$	$\ \mathbf{P} - \mathbf{A}\ _F \downarrow$	$\ \mathbf{P}\mathbf{A}^{-1} - \mathbf{I}\ _F \downarrow$	Time \downarrow	Iterations \downarrow
Prec.	No preconditioner	0.0014	20.70	31 152.94	255.26	1 577.65	30.85	1 153
	Jacobi	0.0003	5.16	31 166.13	205.83	6 319.45	30.12	1 152
	ILU(0)	0.0006	30.32	120 740.90	138.31	3 688.45	3.33	413
Loss	\mathcal{L}_{\max} : Equation (5)	0.0007	5.00	16 139.46	88.76	3 261.23	3.67	437
	\mathcal{L}_{\min} : Equation (6)	1.1375	20 318.88	37 030.72	287.62	50.05	24.41	1 054
	$\hat{\mathcal{L}}_{\min}$: Equation (7)	-	-	-	287.71	50.30	130.01	2 192
	\mathcal{L}_{com} : Equation (8)	0.0017	52.92	66 691.71	197.82	1 240.60	3.42	418

4 Experiments & Results

We evaluate our method on a synthetic dataset of problems arising from the discretization of the Poisson equation. The problem size in our experiments is $n = 2\,500$. We train on 200 and evaluate the results on 10 problem instances. The details for the dataset and implementation can be found in Appendix B.

Comparison of loss functions In Table 1, we present the performance of the learned preconditioner given different loss functions corresponding to the bounds derived in the previous section. We can see that minimizing \mathcal{L}_{\max} and \mathcal{L}_{\min} decrease the largest and increase the smallest singular value of the system respectively and the models achieve the lowest loss for the respective functions. This shows that during training, we are able to minimize the loss functions and by that implicitly optimize the bounds for the singular values.

Optimizing the biased approximation $\hat{\mathcal{L}}_{\min}$ still performs well in terms of decreasing the original loss function corresponding to the bound of the smallest singular value. The resulting preconditioning matrix is highly ill-conditioned for the chosen ϵ parameter leading to numerical instabilities in the inversion of \mathbf{P} and inaccurate results for the singular value decomposition due to the overfitting of the model on the training data.

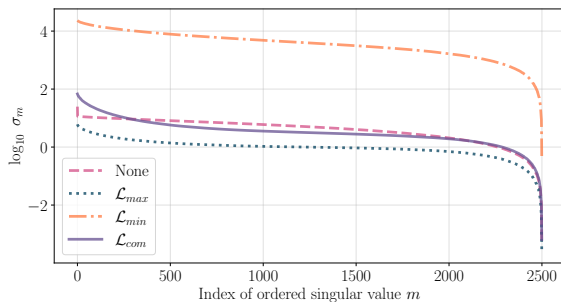


Figure 3. Distribution of singular values of the preconditioned system for different choices of preconditioner.

Optimizing the combined loss \mathcal{L}_{com} reduces both individual loss functions slightly compared to the non-preconditioned case but leads to worse performance on nearly all metrics besides the acceleration of the iterative solver. Additionally, the training of this loss can be numerically unstable as the two loss functions conflict with each other.

Note that, the problem at hand is unbalanced as the spectrum of the original system is already skewed towards small singular values. The performance in terms of GMRES iterations of the different loss functions also depends on the initial distribution of singular values. In Figure 3 we show this distribution for different preconditioners compared to the original distribution.

Comparison with classical preconditioners Additionally, we compare in Table 1 the performance of the learned preconditioner with the classical Jacobi and incomplete LU method without fill-ins, as well as, the case where no preconditioner is applied. In general, the results show the vital importance of selecting an appropriate preconditioner. For the problem considered, ILU and the learned preconditioner perform nearly on par. We can see that even though the conditioning in terms of the largest and smallest singular value of the ILU method is by far inferior to the other preconditioners, it still manages to substantially reduce the number of iterations for convergence.

This shows that the spectrum edges, while important, are not the only factor affecting the method’s efficiency. It underscores the importance of considering the entire spectrum of the preconditioned system when analyzing the method’s convergence.

5 Discussion & Conclusion

In this paper, we learn incomplete factorizations of sparse matrices directly from data. When applied as a preconditioner our approach leads to a significant reduction in terms of iterations compared to the unpreconditioned GMRES. Combining data-driven

methods with existing algorithms has a huge potential since it allows obtaining the best results from both worlds: guarantees about the convergence is obtained from classical analysis of the algorithms while the data-driven components allow us to learn directly from data to improve upon the existing algorithms.

Limitations Our approach assumes having access to a distribution of linear equation systems that share similarities between the problem instances. However, in practice, it is not always trivial to obtain such a distribution of problems. Further, the initial cost of training the network needs to be amortized over many future problems that need to be solved. However, given the initial sample problems, new problems can be solved faster in an online fashion which is important for time-critical applications.

Future work The GNN is designed so that the learned preconditioner matches the sparsity pattern of the input matrix \mathbf{A} . While dynamically learning the sparsity pattern and matrix elements could improve preconditioner quality, the large search space and combinatorial complexity make this challenging.

Our proposed loss function accounts for the spectrum edges in the preconditioned system. However, beyond the edges and condition number, the distribution of singular values also affects the convergence of Krylov subspace methods. Designing loss functions that consider this can further improve the performance of learned preconditioners.

Acknowledgments

We would like to thank Daniel Hernández Escobar and Sebastian Mair for helpful discussions and feedback. This work was supported by the the Göran Gustafsson Foundation and the Wallenberg AI, Autonomous Systems and Software Program (WASP) funded by the Knut and Alice Wallenberg Foundation.

Contribution statement

The idea to apply learned preconditioner to GMRES was initially proposed by JS and later refined together with PH. PH suggested the overall network architecture including the novel activation function to ensure invertibility and derived the theoretical results that were finalized with help of ANJ. ANJ implemented and constructed the initial GNN architecture and the implementation of the GMRES method and came up with the dataset with inputs and support from PH and JS. The final experiments and results were conducted by PH. Writing was primarily done by PH with help of ANJ and inputs from JS.

References

- [1] Y. Saad. *Iterative Methods for Sparse Linear Systems*. Second. Society for Industrial and Applied Mathematics, 2003. DOI: [10.1137/1.9780898718003](https://doi.org/10.1137/1.9780898718003).
- [2] M. Benzi. “Preconditioning techniques for large linear systems: a survey”. In: *Journal of computational Physics* 182.2 (2002), pp. 418–477. DOI: [10.1006/jcph.2002.7176](https://doi.org/10.1006/jcph.2002.7176).
- [3] J. Scott and M. Tuma. *Algorithms for sparse linear systems*. Springer Nature, 2023. DOI: [10.1007/978-3-031-25820-6](https://doi.org/10.1007/978-3-031-25820-6).
- [4] P. Häusner, O. Öktem, and J. Sjölund. “Neural incomplete factorization: learning preconditioners for the conjugate gradient method”. In: *arXiv preprint arXiv:2305.16368* (2023).
- [5] Y. Li, P. Y. Chen, T. Du, and W. Matusik. “Learning preconditioners for conjugate gradient PDE solvers”. In: *International Conference on Machine Learning*. PMLR, 2023, pp. 19425–19439.
- [6] V. Trifonov, A. Rudikov, O. Iliev, I. Oseledets, and E. Muravleva. “Learning from Linear Algebra: A Graph Neural Network Approach to Preconditioner Design for Conjugate Gradient Solvers”. In: *arXiv preprint arXiv:2405.15557* (2024).
- [7] J. Chen. “Graph Neural Preconditioners for Iterative Solutions of Sparse Linear Systems”. In: *arXiv preprint arXiv:2406.00809* (2024).
- [8] M. Bänkestad, J. Andersson, S. Mair, and J. Sjölund. “Ising on the Graph: Task-specific Graph Subsampling via the Ising Model”. In: *arXiv preprint arXiv:2402.10206* (2024).
- [9] M. Li, H. Wang, and P. K. Jimack. “Generative Modeling of Sparse Approximate Inverse Preconditioners”. In: *Computational Science – ICCS 2024*. Cham: Springer Nature Switzerland, 2024, pp. 378–392. DOI: [10.1007/978-3-031-63759-9_40](https://doi.org/10.1007/978-3-031-63759-9_40).
- [10] Y. Saad and M. H. Schultz. “GMRES: A Generalized Minimal Residual Algorithm for Solving Nonsymmetric Linear Systems”. In: *SIAM Journal on Scientific and Statistical Computing* 7.3 (1986), pp. 856–869. DOI: [10.1137/0907058](https://doi.org/10.1137/0907058).
- [11] G. H. Golub and C. F. Van Loan. *Matrix computations*. JHU press, 2013.
- [12] J. W. Pearson and J. Pestana. “Preconditioners for Krylov subspace methods: An overview”. In: *GAMM-Mitteilungen* 43.4 (2020). DOI: [10.1002/gamm.202000015](https://doi.org/10.1002/gamm.202000015).

- [13] T. A. Davis, S. Rajamanickam, and W. M. Sid-Lakhdar. “A survey of direct methods for sparse linear systems”. In: *Acta Numerica* 25 (2016), pp. 383–566. DOI: [10.1017/S0962492916000076](https://doi.org/10.1017/S0962492916000076).
- [14] M. Benzi and M. Tuma. “A comparative study of sparse approximate inverse preconditioners”. In: *Applied Numerical Mathematics* 30.2-3 (1999), pp. 305–340. DOI: [10.1016/S0168-9274\(98\)00118-4](https://doi.org/10.1016/S0168-9274(98)00118-4).
- [15] M. M. Bronstein, J. Bruna, T. Cohen, and P. Veličković. “Geometric Deep Learning: Grids, Groups, Graphs, Geodesics, and Gauges”. In: *arXiv preprint arXiv:2104.13478* (2021).
- [16] P. W. Battaglia, J. B. Hamrick, V. Bapst, A. Sanchez-Gonzalez, V. Zambaldi, M. Malinowski, A. Tacchetti, D. Raposo, A. Santoro, R. Faulkner, et al. “Relational inductive biases, deep learning, and graph networks”. In: *arXiv preprint arXiv:1806.01261* (2018).
- [17] J. Sjölund and M. Bånkestad. “Graph-based neural acceleration for nonnegative matrix factorization”. In: *arXiv preprint arXiv:2202.00264* (2022).
- [18] N. S. Moore, E. C. Cyr, P. Ohm, C. M. Siefert, and R. S. Tuminaro. “Graph neural networks and applied linear algebra”. In: *arXiv preprint arXiv:2310.14084* (2023).
- [19] M. Doob. “Applications of graph theory in linear algebra”. In: *Mathematics Magazine* 57.2 (1984), pp. 67–76. DOI: [10.2307/2689586](https://doi.org/10.2307/2689586).
- [20] Z. Tang, H. Zhang, and J. Chen. “Graph Neural Networks for Selection of Preconditioners and Krylov Solvers”. In: *NeurIPS 2022 Workshop: New Frontiers in Graph Learning*. 2022.
- [21] J. Sappl, L. Seiler, M. Harders, and W. Rauch. “Deep learning of preconditioners for conjugate gradient solvers in urban water related problems”. In: *arXiv preprint arXiv:1906.06925* (2019).
- [22] M. F. Hutchinson. “A stochastic estimator of the trace of the influence matrix for Laplacian smoothing splines”. In: *Communications in Statistics-Simulation and Computation* 18.3 (1989), pp. 1059–1076. DOI: [10.1080/03610919008812866](https://doi.org/10.1080/03610919008812866).
- [23] H. P. Langtangen and A. Logg. “Solving PDEs in minutes-the FEniCS tutorial”. In: *The FEniCS Book* 1 (2016).
- [24] M. Fey and J. E. Lenssen. “Fast graph representation learning with PyTorch Geometric”. In: *arXiv preprint arXiv:1903.02428* (2019).
- [25] N. Nytko, A. Taghibakhshi, T. U. Zaman, S. MacLachlan, L. N. Olson, and M. West. “Optimized sparse matrix operations for reverse mode automatic differentiation”. In: *arXiv preprint arXiv:2212.05159* (2022).
- [26] J. Mayer. “ILU++: A new software package for solving sparse linear systems with iterative methods”. In: *PAMM: Proceedings in Applied Mathematics and Mechanics*. Vol. 7. 1. Wiley Online Library. 2007, pp. 2020123–2020124. DOI: [10.1002/pamm.200700911](https://doi.org/10.1002/pamm.200700911).
- [27] C. Hofreither. *ilupp – ILU algorithms for C++ and Python*. 2020. URL: <https://github.com/c-f-h/ilupp>.

A GMRES algorithm

The right-preconditioned GMRES method is shown in Algorithm A.1. The non-preconditioned version can be obtained by using the identity matrix as a preconditioner ($\mathbf{P} = \mathbf{I}$). Operations where the preconditioner is applied are highlighted for better readability in this section.

Algorithm A.1 RIGHT-PRECONDITIONED GMRES [10]

```

1: Inputs:
2: Non-singular matrix  $\mathbf{A} \in \mathbb{R}^{n \times n}$ 
3: Preconditioner  $\mathbf{P} \in \mathbb{R}^{n \times n}$ 
4: Right-hand side  $\mathbf{b} \in \mathbb{R}^n$ 
5: Initial guess  $\mathbf{x}_0 \in \mathbb{R}^n$ 
6: Tolerance  $\epsilon$  for the residual norm
7: Maximum number of iterations  $k_{\max}$ 
8: Output: Approximate solution  $\mathbf{x}_k$ 
9:  $k = 0$ 
10: ▷ Compute the initial residual
11:  $\mathbf{r}_0 = (\mathbf{b} - \mathbf{A}\mathbf{x}_0)$ 
12:  $\rho_0 = \|\mathbf{r}_0\|_2$ 
13:  $\beta = \rho_0$ 
14: while  $\rho_k > \epsilon\rho_0$  and  $k < k_{\max}$  do
15:    $k \leftarrow k + 1$ 
16:   Arnoldi ( $\mathbf{A}, \mathbf{P}, \mathbf{r}_0, k$ )  $\rightarrow \mathbf{V}_{k+1}, \mathbf{H}_{k+1,k}$ 
17:   Compute the QR factorization of  $\mathbf{H}_{k+1,k}$ 
18:    $\rho_k = |\beta q_{1,k+1}|$ 
19: ▷ Solve using the QR factorization of  $\mathbf{H}_{k+1,k}$ 
20:  $\mathbf{y}_k = \operatorname{argmin}_{\mathbf{y} \in \mathbb{R}^n} \|\beta \mathbf{e}_1 - \mathbf{H}_{k+1,k} \mathbf{y}\|_2$ 
21: ▷ Construct the solution
22:  $\mathbf{x}_k = \mathbf{x}_0 + \mathbf{P}^{-1} \mathbf{V}_k \mathbf{y}_k$ 
23: return  $\mathbf{x}_k$ 

```

Arnoldi method In each step of the iterative scheme (line 16 in Algorithm A.1), the Arnoldi method is used to construct an orthonormal basis of the Krylov subspace \mathcal{K}_k of the current iteration shown in Equation (1). This method is crucial as it ensures that the basis vectors are orthogonal, which in turn allows the GMRES algorithm to efficiently minimize the residual over the Krylov subspace.

For a given number of iterations k , the Arnoldi method (Algorithm A.2) produces an upper Hessenberg matrix $\mathbf{H}_{k,k+1}$, which is related to the matrix \mathbf{A} through the orthonormal basis \mathbf{V}_{k+1} as

$$\mathbf{A}\mathbf{V}_k = \mathbf{V}_{k+1}\mathbf{H}_{k,k+1}, \quad (10)$$

where \mathbf{V}_k consists of the first k columns of \mathbf{V}_{k+1} , forming an orthonormal basis for the Krylov subspace.

Based on the factorization of this basis, the residual and approximate solution can be efficiently obtained by solving a smaller and upper-triangular system derived from the QR factorization of $\mathbf{H}_{k,k+1}$, as shown in line 20 of the GMRES algorithm.

In lines 21–23 of Algorithm A.2, the situation where the element $h_{k+1,k}$ in the upper Hessenberg matrix $\mathbf{H}_{k+1,k}$ becomes zero is addressed. If this condition is met, the loop breaks, indicating that the algorithm has prematurely found an invariant Krylov subspace. When this occurs, the $(k+1)$ -th column of \mathbf{V}_{k+1} does not exist because the last row of $\mathbf{H}_{k+1,k}$ is zero. As a result, Equation (10) simplifies to

$$\mathbf{A}\mathbf{V}_k = \mathbf{V}_k\mathbf{H}_k.$$

This indicates that the Krylov subspace has reached its full dimension, and no further vectors can be generated. Consequently, the GMRES algorithm can terminate early, as the exact solution lies within the current subspace. This premature convergence is referred to as “lucky” because it implies that the solution has been found in less than n iterations.

Also, note that in practice, it is not necessary to run the full Arnoldi algorithm in each iteration but the basis vectors found in the previous iterations can be reused and only the most recent orthonormalization step needs to be executed.

Algorithm A.2 ARNOLDI’S MODIFIED GRAM-SCHMIDT IMPLEMENTATION

```

1: Inputs:
2: Non-singular matrix  $\mathbf{A} \in \mathbb{R}^{n \times n}$ 
3: Preconditioner  $\mathbf{P} \in \mathbb{R}^{n \times n}$ 
4: Initial residual  $\mathbf{r}_0 \in \mathbb{R}^n$ 
5: Number of iterations  $k$ 
6: Outputs:
7: Orthonormal basis  $\mathbf{V}_{k+1} = \{\mathbf{v}_j\}_{j=1}^{k+1}$ ,  $\mathbf{v}_j \in \mathbb{R}^n$ 
8: Hessenberg matrix  $\mathbf{H}_{k+1,k} \in \mathbb{R}^{(k+1) \times k}$ 
9: ▷ Initialize the Arnoldi basis
10:  $\beta = \|\mathbf{r}^{(0)}\|_2$ 
11:  $\mathbf{v}_1 = \beta^{-1}\mathbf{r}^{(0)}$ 
12: for  $i = 1$  to  $k$  do
13:    $\mathbf{w}_{i+1} = \mathbf{A}\mathbf{P}^{-1}\mathbf{v}_i$ 
14:   ▷ Gram-Schmidt ortho-normalization
15:   for  $j = 1$  to  $i$  do
16:      $h_{j,i} = \mathbf{w}_{i+1}^T \mathbf{v}_j$ 
17:      $\mathbf{w}_{i+1} = \mathbf{w}_{i+1} - h_{j,i}\mathbf{v}_j$ 
18:    $h_{i+1,i} = \|\mathbf{w}_{i+1}\|_2$ 
19:   if  $h_{i+1,i} \neq 0$  then
20:      $\mathbf{v}_{i+1} = \mathbf{w}_{i+1}/h_{i+1,i}$ 
21:   else
22:     ▷ Exact solution found (lucky breakdown)
23:     break
24: return  $\mathbf{V}_{k+1}, \mathbf{H}_{k+1,k}$ 

```

Preconditioning The preconditioning matrix \mathbf{P} (or its inverse) does not need to be stored explicitly. Instead, it is sufficient to have access to an implicit representation of the matrix which can be applied to a vector \mathbf{v} to evaluate the product $\mathbf{P}^{-1}\mathbf{v}$ as in line 22 of Algorithm A.1 and Algorithm A.2 respectively.

In the case of preconditioner given by triangular factorizations such as ILU and our learned approach, the matrix is obtained by solving the system $\mathbf{LU}\mathbf{v} = \mathbf{r}$ which can be achieved in $\mathcal{O}(n^2)$ operations using the forward-backward substitution and can be further accelerated by exploiting the sparse structure of the matrices. The solution to solving these systems is equivalent to explicitly inverting the matrices and computing the matrix-vector product $\mathbf{U}^{-1}\mathbf{L}^{-1}\mathbf{r}$ which forms the preconditioning matrix as $\mathbf{P}^{-1} = (\mathbf{LU})^{-1}$. However, solving the triangular systems is more efficient in practice.

B Implementation details

Here, we provide additional details for the implementation of the dataset, our learned preconditioner, and the baseline preconditioners used in the experiments.

B.1 Dataset

Our goal with the provided dataset is not solving a real-world problem. Rather, we focus on a highly ill-conditioned synthetic dataset which allows us to systematically test the different loss functions derived. For the problem scale used, direct methods are much superior compared to the shown results.

Poisson problem The Poisson equation is an elliptic partial differential equation (PDE) and one of the most fundamental problems in numerical computational science [23]. The general form of the Poisson equation is given by:

$$\begin{aligned} -\nabla^2 u(x) &= f(x) & x \in \Omega, \\ u(x) &= u_D(x) & x \in \partial\Omega, \end{aligned} \quad (11)$$

where $f(x)$ is the source function and $u(x)$ is the unknown function to be solved for.

In our study, we generate the matrix \mathbf{A} using `pyang.gallery.poisson`, which implicitly assumes unit spacing and Dirichlet boundary conditions, typically set to zero. The right-hand side of the linear equation system, \mathbf{b} , is derived from the source function $f(x, y) = \sin(\pi x)\sin(\pi y)$. By discretizing the problem using the finite element method, we obtain a system of linear equations of the form $\mathbf{Ax} = \mathbf{b}$, where the stiffness matrix \mathbf{A} is sparse and symmetric positive definite. Throughout our experiments, we use matrices of size $n = 2500$.

Noisy data However, we are not specifically interested in spd matrices. Therefore, to obtain a distribution \mathbb{A} over a large number of Poisson equation PDE problems that can be efficiently solved using GMRES, we perturb all the nonzero entries with standard Gaussian noise, which yields arbitrary matrices not necessarily spd. Let us denote the perturbed matrix as $\mathbf{A}' = (a'_{ij})$.

We can represent this mathematically by:

$$a'_{ij} = \begin{cases} a_{ij} + X_{ij} & \text{if } a_{ij} \neq 0, \\ 0 & \text{if } a_{ij} = 0, \end{cases}$$

where $X_{ij} \sim \mathcal{N}(0, 1)$ are i.i.d. random variables.

By introducing randomness into \mathbf{A} , we are effectively modeling a scenario where the system’s properties are not perfectly regular, which could represent, for example, some form of physical or numerical irregularity or perturbation in the grid or medium. During testing, we use a deterministic right-hand side \mathbf{b} as described previously. However, for the supervised training dataset we sample the vectors \mathbf{b} to be normally distributed in order to avoid overfitting as this would lead to a significant decrease in model performance.

Problem instances All problem instances generated come from the same distribution but using non-overlapping random seeds we ensure that there is no data leakage between the training and test data. We create 200 problem instances for training and 10 instances for validation and testing respectively.

All problems are of size $n = 2500$ with approximately 50 000 – 150 000 non-zero elements. The condition number κ of the unpreconditioned system is in the range between 5 000 to 50 000. Thus, even though the problem parameters only vary slightly, the resulting conditioning and potential performance of the different loss functions can be very different between the individual problem instances.

B.2 Network architecture

We implement the neural network based on the `pytorch-geometric` framework which offers direct support for computing the node features and utility functions such as adding remaining self-loops [24]. During inference, we utilize the `numml` sparse matrix package to efficiently compute the forward-backward substitution [25]. The pseudocode for the forward pass of the learned preconditioner is shown in Algorithm B.1.

Inputs and transformations As described in Section 3, we transform the original linear equation system matrix \mathbf{A} into a graph \mathcal{G} using the Coates graph representation. We use the nonzero elements of the matrix as edge features and add a second edge feature as a positional encoding of the output. For the node features, we utilize the same set of 8 input features as previously applied by Häusner et al. [4] describing the structural properties of the matrix.

Message-passing network In our implementation, we use $L = 3$ message-passing steps. We define a hidden size of $n = 32$ for the edge embeddings and $m = 16$ for the node embeddings in the hidden layers of the neural network allowing for sufficient flexibility

Algorithm B.1 PSEUDO-CODE FOR THE LEARNED LU FACTORIZATION PRECONDITIONER

- 1: **Input:** Coates graph representation $\mathcal{G} = (\mathcal{V}, \mathcal{E})$ of the system matrix \mathbf{A} .
- 2: **Output:** Lower and upper triangular matrices \mathbf{L} and \mathbf{U} of the learned factorization.
- 3: \triangleright *Input transformations:*
- 4: Add remaining self-loops to the graph \mathcal{G} .
- 5: Compute node features $\mathbf{n}_i \in \mathbb{R}^8$.
- 6: Compute edge features $\mathbf{e}_{ij} \in \mathbb{R}^2$.
- 7: \triangleright *Message passing layers*
- 8: **for** $l \in \{0, 1, \dots, L - 1\}$ **do**
- 9: **for** $(i, j) \in \mathcal{E}$ **do**
- 10: \triangleright *Compute updated edge features*
- 11: $\mathbf{e}_{ij}^{l+1} = \psi_{\theta}(\mathbf{e}_{ij}^l, \mathbf{n}_i^l, \mathbf{n}_j^l)$
- 12: **for** $i \in \{1, \dots, n\}$ **do**
- 13: \triangleright *Aggregate edge features per node*
- 14: $\mathbf{m}_i^{l+1} = \bigoplus_{j \in \mathcal{N}(i)} \mathbf{e}_{ji}^{l+1}$
- 15: \triangleright *Compute updated node features*
- 16: $\mathbf{n}_i^{l+1} = \phi_{\theta}(\mathbf{n}_i^l, \mathbf{m}_i^{l+1})$
- 17: **if** not final layer in the network **then**
- 18: \triangleright *Add skip connections*
- 19: **for** $(i, j) \in \mathcal{E}$ **do**
- 20: $\mathbf{e}_{ij}^{l+1} \leftarrow [\mathbf{e}_{ij}^{l+1}, a_{ij}]^{\top}$
- 21: \triangleright *Form the lower triangular matrix $\mathbf{L} = (l_{ij})$*

$$(l_{ij}) \leftarrow \begin{cases} e_{ij}^{(L)}, & \text{if } (i, j) \in \mathcal{E} \text{ and } i > j, \\ 0, & \text{otherwise} \end{cases}$$
- 22: \triangleright *Form the upper triangular matrix $\mathbf{U} = (u_{ij})$*

$$(u_{ij}) \leftarrow \begin{cases} e_{ij}^{(L)}, & \text{if } (i, j) \in \mathcal{E} \text{ and } i < j, \\ 0, & \text{otherwise} \end{cases}$$
- 23: \triangleright *Ensure invertibility*
- 24: **for** $i \in \{1, \dots, n\}$ **do**
- 25: $l_{ii} \leftarrow \zeta(e_{ii}^{(L)})$
- 26: $u_{ii} \leftarrow 1$
- 27: **return** (\mathbf{L}, \mathbf{U})

in the network’s parameterization. The incoming messages at each node are aggregated using the mean aggregation function, which ensures a balanced contribution from neighboring nodes. Thus, our GNN has a total of 4889 parameters to train.

Output The final edge embedding is chosen to be scalar by designing the edge update function to produce a single output, i.e. $e_{ij}^{(L)} \in \mathbb{R}$, allowing us to directly transform the output into a lower- and upper-triangular matrix. We enforce the diagonal elements of \mathbf{U} to be ones and apply the activation function ϕ from Equation (3) to the diagonal elements of \mathbf{L} . Note that during training, we instead use the approximation $\hat{\phi}$ from Equation (4) in line 25 as discussed in the main text.

Training Our model is trained on the dataset of

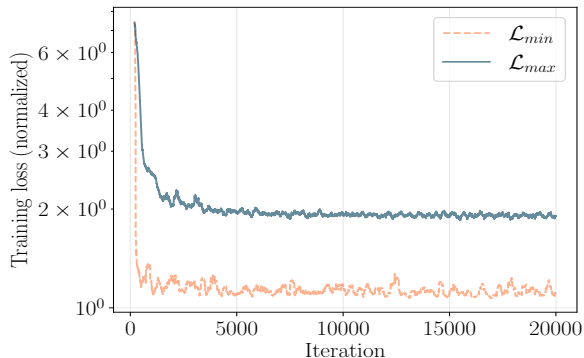


Figure B.1. Normalized training loss using different loss functions from Section 3.

200 problem instances of size $n = 2500$ for 100 iterations. The best-performing model during the training based on the validation GMRES performance is chosen in order to avoid overfitting. As a validation metric, we use the number of GMRES iterations of the learned preconditioner on the validation data as this is the downstream metric of interest.

We use an NVIDIA-A100 GPU with 80 GB of memory for training. Each epoch, consisting of 200 parameter update steps using the Adam optimizer with a learning rate of 0.001 and a batch size of 1, requires 2 seconds. Thus, the total time required for model training is approximately 5 minutes. Further during training we use gradient clipping with parameter 1. We assume throughout that a supervised dataset is readily available and we do not need to create samples for the loss function Equation (7) before the training process. We use the right-hand sides \mathbf{b} are generated as described in Section B.1.

For loss functions that require solving the system $\mathbf{A}^{-1}\mathbf{w}$, training takes significantly longer with approximately 20 minutes. However, solving the systems can be implemented efficiently for the problem scale that we consider in our experiments.

Tuning We only conducted a minimal level of hyper-parameter tuning for the model architecture. Tuning the loss function in Equation (8), optimization of the objective becomes numerically more difficult as the two terms are in conflict with each other. We choose the hyper-parameter $\alpha = \frac{1}{5}$ based on the validation set performance to balance out the two loss terms of the combined loss.

B.3 Baselines

The GMRES algorithm and the Arnoldi method, given in Algorithm A.1 and Algorithm A.2, respectively, are implemented in `pytorch` directly.

The Jacobi preconditioner can be implemented and applied very efficiently using `pytorch` sparse data structures for diagonal matrices. For the ILU(0) preconditioner, we use the ILU++ implemen-

tation which is a high-performance implementation of the algorithm in C++ [26, 27].

During inference, we run all operations – including the neural network-driven preconditioner – on the CPU in order to ensure a fair comparison between the different methods. For all methods, the time it takes to compute the preconditioner can be neglected compared to the time required for the GMRES algorithm.

C Proofs

In the following section, we prove the lemmas from the main text. The proofs can easily be verified and rely on basic norm transformations and inequalities.

Proof of Lemma 1 In the first lemma, we are interested in obtaining an upper bound on the largest singular value of the preconditioned linear system. This allows our loss function to minimize an upper bound on the large end of the spectrum of the preconditioned system.

$$\begin{aligned}\sigma_{\max}(\mathbf{A}\mathbf{P}^{-1}) &= \|\mathbf{A}\mathbf{P}^{-1}\|_2 \\ &= \|(\mathbf{A} - \mathbf{P} + \mathbf{P})\mathbf{P}^{-1}\|_2 \\ &= \|(\mathbf{A} - \mathbf{P})\mathbf{P}^{-1} + \mathbf{I}\|_2 \\ &\leq \|(\mathbf{A} - \mathbf{P})\mathbf{P}^{-1}\|_2 + \|\mathbf{I}\|_2 \\ &\leq \|\mathbf{A} - \mathbf{P}\|_2 \|\mathbf{P}^{-1}\|_2 + 1\end{aligned}$$

Now, we exploit the structure of the learned preconditioner to obtain an upper bound for $\|\mathbf{P}^{-1}\|_2$. Specifically, we use two key observations. First, the matrix \mathbf{U} has ones on the diagonal. Second, the absolute values of the diagonal elements on the matrix \mathbf{L} are bounded from below by ϵ , a property that arises from the specific choice of activation function in Equation (3).

These properties, when combined with the fact that the singular values of a triangular matrix coincide with the absolute value of its diagonal elements, allow us to derive the following upper bound on the spectral norm of the preconditioner \mathbf{P} :

$$\begin{aligned}\|\mathbf{P}^{-1}\|_2 &= \|\mathbf{U}^{-1}\mathbf{L}^{-1}\|_2 \\ &\leq \|\mathbf{U}^{-1}\|_2 \|\mathbf{L}^{-1}\|_2 \\ &= \frac{1}{\sigma_{\min}(\mathbf{U})} \cdot \frac{1}{\sigma_{\min}(\mathbf{L})} \\ &\leq \epsilon^{-1}.\end{aligned}$$

Combining this bound on $\|\mathbf{P}^{-1}\|_2$ with the previous inequality, we obtain:

$$\sigma_{\max}(\mathbf{A}\mathbf{P}^{-1}) \leq \epsilon^{-1}\|\mathbf{A} - \mathbf{P}\|_2 + 1.$$

Proof of Lemma 2 In the second Lemma, we show how to obtain a lower bound on the smallest singular

value of the preconditioned system. Our goal is to maximize this bound as it allows us to increase the small singular values of the preconditioned system.

$$\begin{aligned}\sigma_{\min}(\mathbf{A}\mathbf{P}^{-1}) &= \frac{1}{\sigma_{\max}(\mathbf{P}\mathbf{A}^{-1})} \\ &= \frac{1}{\|\mathbf{P}\mathbf{A}^{-1}\|_2} \\ &\geq \frac{1}{\|\mathbf{P}\mathbf{A}^{-1}\|_F}\end{aligned}$$

Previous learned preconditioner approaches in the literature [5, 6] used the following additional steps to obtain a weaker bound on the smallest singular value of the system:

$$\begin{aligned}\|\mathbf{P}\mathbf{A}^{-1}\|_2 &= \|\mathbf{P}\mathbf{A}^{-1}\|_2 - 1 + 1 \\ &= \|\mathbf{P}\mathbf{A}^{-1}\|_2 - \|\mathbf{I}\|_2 + 1 \\ &\leq \|\mathbf{P}\mathbf{A}^{-1}\|_2 - \|\mathbf{I}\|_2 + 1 \\ &\leq \|\mathbf{P}\mathbf{A}^{-1} - \mathbf{I}\|_2 + 1 \\ &\leq \|\mathbf{P}\mathbf{A}^{-1} - \mathbf{I}\|_F + 1.\end{aligned}$$

The reason for this is that optimizing first approximation directly leads to degenerate solutions as the minimum is attained when $\mathbf{P} \approx 0$ which would avoid having small singular values but the large singular value of the preconditioned system would be unbounded. Therefore, one can see the additional term involving \mathbf{I} as a regularizer enforcing \mathbf{P} to be non-degenerate.

Frobenius norm approximation Equivalently to optimizing over the Frobenius norm, we can optimize the preconditioner over the squared Frobenius norm instead as we are only interested in the best parameters, not the best objective value. This has the additional advantage that the loss function is fully differentiable. Further, we can approximate the squared Frobenius norm using Hutchinson’s trace estimator which can be easily verified [22]. For a random vector \mathbf{w} that satisfies $\mathbb{E}[\mathbf{w}\mathbf{w}^T] = \mathbf{I}$ we can approximate the squared Frobenius norm using the following transformations:

$$\begin{aligned}\|\mathbf{M}\|_F^2 &= \text{trace}(\mathbf{M}^T\mathbf{M}) \\ &= \text{trace}(\mathbf{M}^T\mathbf{M}\mathbb{E}[\mathbf{w}\mathbf{w}^T]) \\ &= \mathbb{E}[\text{trace}(\mathbf{M}^T\mathbf{M}\mathbf{w}\mathbf{w}^T)] \\ &= \mathbb{E}[\text{trace}(\mathbf{w}^T\mathbf{M}^T\mathbf{M}\mathbf{w})] \\ &= \mathbb{E}[\mathbf{w}^T\mathbf{M}^T\mathbf{M}\mathbf{w}] \\ &\approx \mathbf{w}^T\mathbf{M}^T\mathbf{M}\mathbf{w} \\ &= \|\mathbf{M}\mathbf{w}\|_2^2\end{aligned}$$

In practice, \mathbf{w} is typically chosen to follow either a standard normal distribution or a Rademacher distribution.

While it is possible to use multiple samples to obtain a more accurate approximation of the

Frobenius norm, we follow previous approaches by estimating the norm using a single random vector to limit computational resources.

D Additional results

Here, we provide additional results for the baseline and learned preconditioners. In Figure D.1, we show the singular value distribution of the baseline preconditioners for the same problem as previously shown in Figure 3.

We can see that even though the ILU preconditioner has a few very large singular values, most values are clustered around 1. This leads to a very fast convergence as observed in Table 1 even though the condition number κ of the problem is very high.

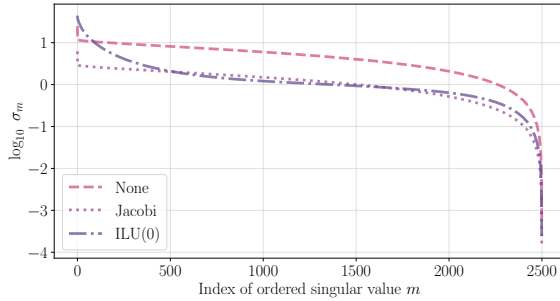


Figure D.1. Distribution of singular values of the preconditioned system for different choices of baseline preconditioner.